

See discussions, stats, and author profiles for this publication at: <https://www.researchgate.net/publication/235563173>

# Excitations of liquid<sup>4</sup>He in disorder and boson localization

Article in *Physical review. B, Condensed matter* · January 2004

DOI: 10.1103/PhysRevB.69.014514

---

CITATIONS

21

---

READS

38

6 authors, including:



**David Daughton**

Lake Shore Cryotronics

29 PUBLICATIONS 109 CITATIONS

SEE PROFILE



**Norbert Mulders**

University of Delaware

165 PUBLICATIONS 1,435 CITATIONS

SEE PROFILE

Some of the authors of this publication are also working on these related projects:



PhD Elementary Excitations of Liquid 4He in porous media [View project](#)

# Excitations of liquid $^4\text{He}$ in disorder and boson localization

Francesco Albergamo\*

*Institut Laue-Langevin, Boîte Postale 156, 38042 Grenoble, France  
and Istituto Nazionale di Fisica della Materia, Unità dell'Aquila, Italy*

Henry R. Glyde,<sup>†</sup> David R. Daughton,<sup>‡</sup> and Norbert Mulders<sup>§</sup>

*Department of Physics and Astronomy, University of Delaware, Newark, Delaware 19716-2570, USA*

Jacques Bossy<sup>||</sup>

*Centre de Recherche sur les Très Basses Températures, CNRS, Boîte Postale 166, 38042 Grenoble Cedex 9, France*

Helmut Schober<sup>¶</sup>

*Institut Laue-Langevin, Boîte Postale 156, 38042 Grenoble, France*

(Received 16 September 2003; published 29 January 2004)

We present neutron-scattering measurements of the excitations of liquid  $^4\text{He}$  confined in Vycor glass focusing on wavevectors in the range  $1.55 \text{ \AA}^{-1} \leq Q \leq 1.80 \text{ \AA}^{-1}$  and temperatures around the superfluid—normal fluid critical temperature  $T_c$ .  $^4\text{He}$  adsorption isotherms have been measured on the Vycor sample in order to control filling. The superfluid density of  $^4\text{He}$  in the sample was measured using a sound velocity technique yielding a superfluid to normal fluid critical temperature of  $T_c = 2.05 \text{ K}$  at full filling. The liquid  $^4\text{He}$  in Vycor supports well-defined phonon-roton excitations above the critical temperature in Vycor suggesting the existence of localized Bose-Einstein condensation (BEC) in the normal phase above  $T_c$ . The phonon-roton excitations (localized BEC) appear to exist up to temperatures of  $T_\lambda = 2.17 \text{ K}$ . At full filling the phonon-roton excitations have energies that are the same as those in bulk superfluid  $^4\text{He}$  within precision. The liquid also supports layer modes for wave vectors in the roton region ( $1.90 \text{ \AA}^{-1} \leq Q \leq 2.10 \text{ \AA}^{-1}$ ) as observed previously in Vycor, aerogel, MCM, and Geltech silica.

DOI: 10.1103/PhysRevB.69.014514

PACS number(s): 67.40.Db, 64.70.Ja, 61.12.Ex

## I. INTRODUCTION

The impact of disorder on Bose-Einstein condensation (BEC), on superfluidity, and on the elementary excitations of Bose systems is a topic of great current interest.<sup>1–9</sup> Recent experimental examples of bosons in disorder are alkali atoms in traps combined with optical lattices or molecular impurities and liquid  $^4\text{He}$  confined in porous media.<sup>4,10–17</sup> Other examples are Cooper pairs in high- $T_c$  materials,<sup>18</sup> flux lines in type II superconductors,<sup>19–21</sup> disordered thin films,<sup>22</sup> and Josephson-Junction arrays.<sup>23,24</sup>

Model calculations of BEC and superfluidity in a dilute Bose gas containing disorder at  $T=0 \text{ K}$  find that disorder reduces superfluid density  $\rho_s(T)$  more than the condensate fraction,  $n_0(T)$ .<sup>3</sup> This result has been impressively extended to dense Bose liquids using Monte Carlo techniques.<sup>8</sup> Indeed for strong enough static disorder the superfluid density can be reduced below the condensate fraction. Model calculations of BEC and superfluidity in a dilute Bose gas in disorder at finite temperature suggest that  $T_c$  is suppressed below  $T_{\text{BEC}}$  by disorder.<sup>9</sup> Conceivably, therefore, with an increase in temperature, a state could be reached where the macroscopic superfluidity and  $\rho_s(T)$  have gone to zero but the condensate fraction, at least in some regions of the system, is still finite. In this event, we could have regions of BEC with no superfluidity across the sample. In this case, disorder would separate the superfluid to normal fluid critical temperature,  $T_c$ , from the critical temperature for BEC,  $T_{\text{BEC}}$ , with  $T_c < T_{\text{BEC}}$ .

Specifically, disorder can also localize BEC. Model studies and simulations have demonstrated that the condensate can be isolated to specific regions by disorder.<sup>2,25</sup> Similarly, in superconductors regions of superconductivity where there is a finite energy gap can be localized by disorder<sup>18</sup> and perhaps be fluctuating in time. In these models there can be a temperature region or a level of disorder in which the condensate is localized to favorable regions. These islands of condensate are separated by regions of normal fluid. In this circumstance, there is phase coherence over short length scales in local regions only. Observable superflow across the sample appears at a lower temperature where the islands of BEC are larger and become connected so that there is phase coherence across the whole sample.

In recent neutron-scattering experiments, we have observed evidence that there is localized BEC above the superfluid-normal transition temperature,  $T_c$ , of liquid  $^4\text{He}$  in porous media. Specifically, we observe phonon-roton (P-R) excitations above  $T_c$  in liquid  $^4\text{He}$  in Vycor<sup>15,26</sup> and Geltech silica<sup>27</sup> (for comment see Refs. 16 and 28). Since observable P-R excitations at wave vectors  $Q \geq 1 \text{ \AA}^{-1}$  arise because there is a condensate, this shows that there must be a condensate above  $T_c$ , at least in some regions in the media. At the same time, since the excitations at higher  $Q$  have short wavelengths, the dimensions of the regions could be quite small. In these porous media, the regions of BEC might be expected to have coherence lengths of 20–50  $\text{\AA}$ . To date only three temperatures above  $T_c$  in two samples have been investigated.

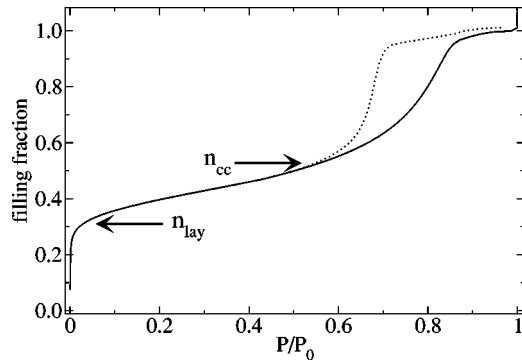


FIG. 1. Adsorption isotherms of  $^4\text{He}$  in the present Vycor sample at  $T=2.40\pm 0.01$  K.  $P/P_0$  is the ratio of measured pressure  $P$  to the saturated vapor pressure of bulk  $^4\text{He}$  at  $T=2.40$  K,  $P_0$ . The solid line shows the adsorption branch; the dotted line shows desorption branch. Full filling is at  $6\text{ mmol g}^{-1}$ .  $n_{\text{lay}}$  indicates the filling at which the “dead” (solid) layers on the Vycor surface are completed,  $n_{\text{cc}}$  the filling at which capillary condensation filling begins.

In this context we have made inelastic neutron-scattering measurements of the P-R excitations of liquid  $^4\text{He}$  in a specially prepared sample of Vycor at several temperatures near  $T_c$  and above  $T_c$ . We have also made a separate superfluid density measurement of this sample. The superfluid–normal fluid transition temperature of this sample is found to be  $T_c = 2.05$  K. The present results show that there are well-defined and clearly observable P-R excitations above  $T_c$ . The excitations are observed up to  $T_\lambda = 2.17$  K. Specifically, right at  $T_c = 2.05$  K for this sample there are clearly observable P-R modes with  $\approx 40\%$  of the observed scattered intensity in the P-R mode. The weight of the P-R mode at wave vectors  $Q \gtrsim 1.5\text{ \AA}^{-1}$  scales with  $T$  approximately with  $\rho_s(T)$  in bulk liquid  $^4\text{He}$  and vanishes approximately at  $T_\lambda$ . We have also recently reported direct measurements of the condensate fraction in the present Vycor sample.<sup>29</sup> While these measurements show that there is definitely a condensate in  $^4\text{He}$  in Vycor, the critical temperature for BEC is not well determined.

In Secs. II and III we describe the sample, the neutron-scattering measurements and the model that was fitted to the observed data, respectively. The results are presented and discussed in Secs. IV and V, respectively.

## II. EXPERIMENT

### A. Sample synthesis and characterization

The Vycor sample was synthesized at Corning Glass by P. S. Danielson using 99.95%  $^{11}\text{B}$  enriched  $\text{B}_2\text{O}_3$  to reduce neutron absorption arising from  $^{10}\text{B}$ . After cutting, the samples were dried at  $350^\circ\text{C}$  in flowing helium gas and thereafter kept under a helium atmosphere.

We made adsorption isotherm measurements on 223 mg of the sample used for the neutron-scattering experiment [mass  $m = 11.393(1)$  g and dimensions  $(44.2 \times 10.0 \times 16.8)$  mm<sup>3</sup>] as shown in Fig. 1. The adsorption diagram is interpreted as follows. For reduced pressure  $p$ , defined as the

TABLE I. Experimental conditions for the neutron-scattering experiment. FF is the amount of helium adsorbed in Vycor expressed in filling fraction units. Typical errors on the sample temperature  $T$ , filling fraction, and relative pressure  $P/P_0$  are 0.01 K, 0.005, and 0.01, respectively.

$T$ (K)	0.30	0.39	1.80	1.95	2.05	2.15	2.25	2.40
FF	0.000	0.826	0.914	0.932	0.893	0.878	0.870	0.871
$P/P_0$	n/a	n/a	0.85	0.95	0.69	0.71	0.73	0.75

ratio of measured pressure  $P$  to the saturated vapor pressure  $P_0$ ,  $p \equiv P/P_0 < 0.05$ , the helium entering the pores is tightly bound to the Vycor surface, probably forming solid layer(s) on the substrate. Further helium entering the pores up to a reduced pressure  $p \approx 0.6$  is interpreted as completing or forming one or more layer(s) that remain liquid. For  $p \gtrsim 0.6$ , the helium coalesces in the liquid state within the pores yielding the so-called capillary condensation (here between  $p \approx 0.60$  and  $p \approx 0.85$ ). Further adsorption is believed to occur in larger pores. The sample used in the neutron scattering experiment was at pressure slightly below SVP as indicated in Table I.

### B. Neutron-scattering experiment

The neutron-scattering data were taken on the IN6 time-of-flight spectrometer at the Institut Laue-Langevin, Grenoble, France, using an incident neutron wavelength of  $\lambda = 4.62\text{ \AA}$ . Measurements were conducted at several temperatures ranging from  $T = 0.30$  K to  $T = 2.40$  K, obtained in a  $^3\text{He}$  cryostat. The aluminum thermal screens of the cryostat were covered by Cd shields to lower the noise due to reflections. The sample was held in an aluminum tube (inner diameter  $d_i = 20$  mm, outer diameter  $d_o = 24$  mm, height  $h = 65$  mm) which had its upper and lower parts masked by Cd shields. The filling of the Vycor was slightly different at each temperature, due mainly to change of the equilibrium pressure in the sample cell.

### C. Data reduction

A summary of the temperatures investigated and the filling of the Vycor at each temperature is presented in Table I. The scattering intensity from the empty Vycor sample plus can was determined at  $T = 0.30$  K, as indicated in Table I. This was subtracted from the intensity observed for filled Vycor. The resulting net intensity observed at each temperature was arranged in  $Q$  bins of width  $0.05\text{ \AA}^{-1}$  in the range  $0.55\text{ \AA}^{-1} < Q < 2.15\text{ \AA}^{-1}$ . Examples of the resulting net scattering intensity,  $S_E(Q, \omega; T)$ , at four wave vectors and several temperatures are shown in Fig. 2. In order to compare  $S(Q, \omega; T)$  at different temperatures, we must compare scattering intensities for the same quantity of liquid  $^4\text{He}$  at each temperature. However, as noted in Table I, the fillings differed somewhat at different temperatures. To correct for this small difference we normalized the function fitted to the data to a given amount  $n_L$  of liquid  $^4\text{He}$  at each temperature.

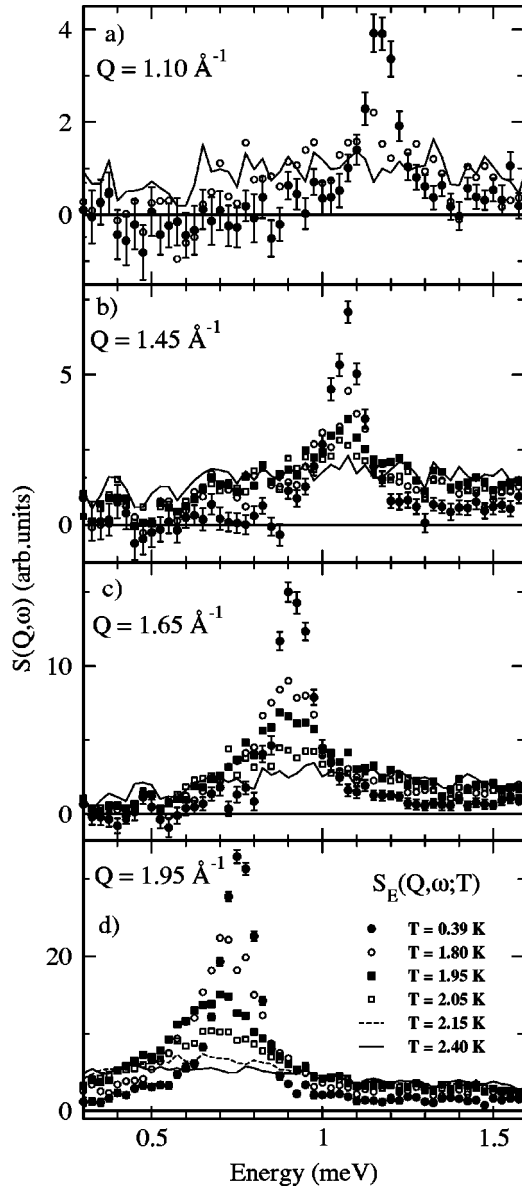


FIG. 2. Net scattering intensity from liquid  $^4\text{He}$  in Vycor. Each subpanel shows spectra at several temperatures at the indicated  $Q$  value.

As discussed in Sec. II A and shown in Fig. 1, the  $^4\text{He}$  for fillings up to  $n_{\text{lay}}$  forms “dead” solid layers on the Vycor surface that do not support phonon-roton modes. Similarly, from a previous study on  $^4\text{He}$  confined in MCM-41,<sup>30</sup> we found that up to a filling corresponding to the beginning of capillary condensation,  $n_{\text{cc}}$  in Fig. 1, the liquid layers formed or completed on the top of the first solid layers still do not support a three-dimensional (3D) phonon-roton mode. The well-known elementary excitation spectrum becomes measurable once the capillary condensation has started (fillings above  $n_{\text{cc}}$ ). At each temperature we assumed that the amount of liquid  $^4\text{He}$  that contributes to the phonon-roton intensity is  $n_{\text{L}} = n_{\text{ads}} - n_{\text{cc}}$  where  $n_{\text{ads}}$  is the adsorbed amount at that temperature. We also test this assumption later in the manuscript, when determining the fraction  $f_{\text{S}}(T)$  of the intensity

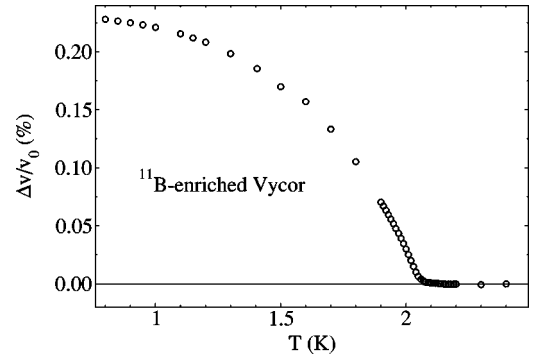


FIG. 3. Sound speed variation as a function of temperature in the present sample of Vycor filled with  $^4\text{He}$  at SVP.

in the P-R mode, by using  $n_{\text{L}} = n_{\text{ads}} - n_{\text{lay}}$  (see Fig. 14) and find that the results are largely unchanged.

#### D. Superfluid density measurements

The superfluid to normal fluid transition temperature,  $T_{\text{c}}$ , has been measured by an ultrasonic technique.<sup>31</sup> We used a frequency of 7.64 MHz on a sample that was 13.0 mm long. The transverse sound speed in the empty Vycor sample was 2320 m/s. The sample was completely filled with  $^4\text{He}$  at saturated vapor pressure. Results for the sound speed relative variation,  $\Delta v/v$ , are shown in Fig. 3. We find a transition temperature of  $T_{\text{c}} = 2.05$  K, somewhat higher than the often quoted<sup>32</sup>  $T_{\text{c}}$  for  $^4\text{He}$  in Vycor (about 1.95 K). The transition temperature in literature is found to vary from sample to sample ranging from about 1.94 (Ref. 31) to 2.03 K (Ref. 33).

### III. MODEL AND FITTING

An aim of these measurements was to test whether the dynamic structure factor of confined helium at temperature  $T$  can be represented as a sum of a “singular,” phonon-roton excitation component,  $S_{\text{S}}(Q, \omega; T)$ , weighted by a temperature-dependent factor,  $f_{\text{S}}(T)$ , plus a “normal” component,  $S_{\text{N}}(Q, \omega)$ :

$$S(Q, \omega; T) = f_{\text{S}}(T)S_{\text{S}}(Q, \omega; T) + [1 - f_{\text{S}}(T)]S_{\text{N}}(Q, \omega). \quad (1)$$

The goal is to determine  $f_{\text{S}}(T)$  and particularly the temperature at which  $f_{\text{S}}(T)$  goes to zero.

The singular component is assumed to arise from the existence of a condensate in the liquid (as does the superfluid density). The normal component is assumed to be the  $S(Q, \omega)$  of normal liquid  $^4\text{He}$ . In bulk normal liquid  $^4\text{He}$  at temperatures  $T > T_{\lambda}$ ,  $S(Q, \omega)$  is found to be a broad function of  $\omega$  and largely independent of  $T$ . Similarly, we found the present  $S(Q, \omega)$  in Vycor to be largely independent of  $T$  for  $T \geq 2.15$  K (e.g., see Figs. 2 and 10). Similarly, given the present instrument resolution (100  $\mu\text{eV}$ ), we find that  $S(Q, \omega)$  folded with the instrument resolution changes little with  $T$  below  $T \approx 1$  K.

The singular component is usually<sup>34,35</sup> taken to be the sum of a sharply peaked “single excitation” component

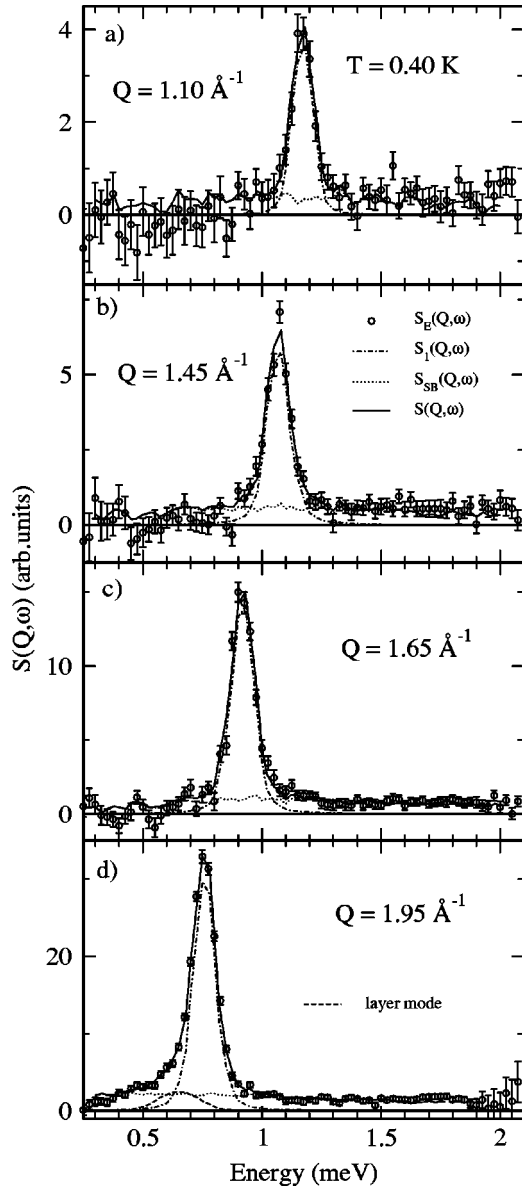


FIG. 4. Dynamic structure factor,  $S(Q, \omega)$ , of liquid  $^4\text{He}$  in Vycor at  $T = 0.4$  K.  $S(Q, \omega)$  at  $T = 0.39$  K is represented as the sum of single excitation and background components,  $S(Q, \omega) = S_1(Q, \omega) + S_{SB}(Q, \omega)$  as in Eqs. (1) and (2) with  $f_S(T) = 1$ . At  $Q = 1.95 \text{ \AA}^{-1}$ , an additional Gaussian component, representing the layer mode, has been included in the fit to the data.

$S_1(Q, \omega; T)$ , plus a broad “multiple excitation” component,  $S_M(Q, \omega; T)$ .  $S_M(Q, \omega; T)$  contributes at energies higher than the single excitation energy. In the present measurements, we find that  $S_M(Q, \omega; T)$  at low temperature could not be distinguished from a broad “background” scattering intensity which contributes at all energies (e.g., see Fig. 4). Thus we replace  $S_M(Q, \omega; T)$  by a broad “background” term  $S_{SB}(Q, \omega)$ , which was assumed to be independent of  $T$ , and write

$$S_S(Q, \omega; T) = S_1(Q, \omega; T) + S_{SB}(Q, \omega). \quad (2)$$

Substituting Eq. (2) into Eq. (1), the function we fit to the data can be written as

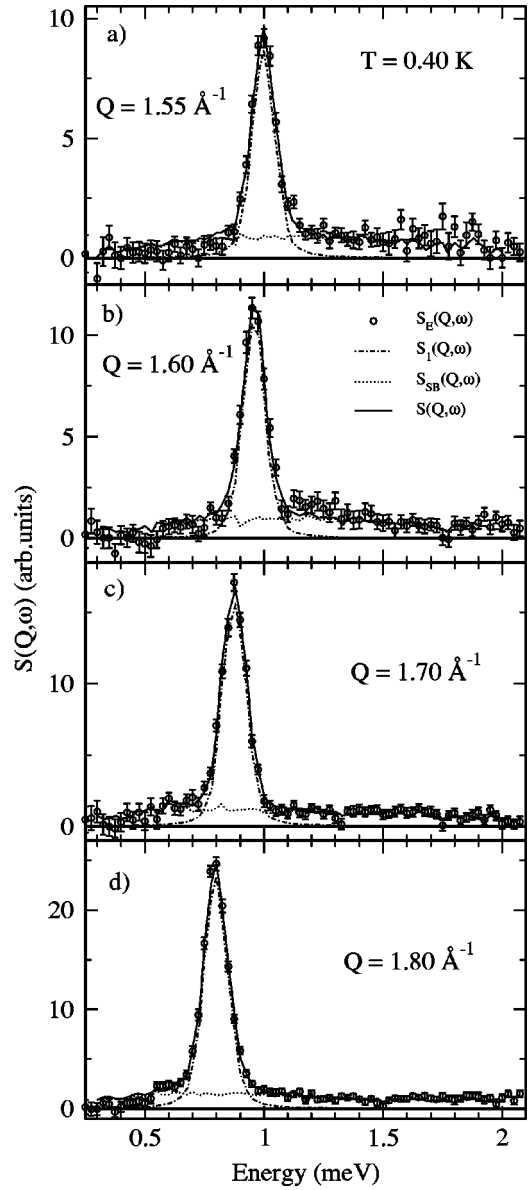


FIG. 5. Same as Fig. 4, for  $Q$  range  $1.55 \text{ \AA}^{-1} \leq Q \leq 1.80 \text{ \AA}^{-1}$ .

$$S(Q, \omega; T) = f_S(T)S_1(Q, \omega; T) + S_B(Q, \omega; T), \quad (3)$$

where

$$S_B(Q, \omega; T) = f_S(T)S_{SB}(Q, \omega) + (1 - f_S(T))S_N(Q, \omega). \quad (4)$$

Here,  $S_B(Q, \omega; T)$  is a broad function of  $\omega$  with temperature dependence given entirely by  $f_S(T)$ .

To implement the model we assume that at  $T = 0.39$  K,  $S(Q, \omega; T) = S_S(Q, \omega; T)$ , that is,  $f_S(0.39) = 1$  and at  $T = T_N$ ,  $S(Q, \omega; T) = S_N(Q, \omega)$ , that is,  $f_S(T_N) = 0$ . Here  $T_N$  is a temperature in the normal phase at which the singular component is taken to be zero. With this assumption, we take  $S_N(Q, \omega)$  as  $S_E(Q, \omega; T_N)$ , the observed net intensity at a temperature  $T_N \approx T_\lambda$ :

$$S_N(Q, \omega) = S_E(Q, \omega; T_N). \quad (5)$$

To test that the eventual results were independent of reasonable choice of  $T_N$ ,  $S_E(Q, \omega; T_N)$  at three values of  $T_N$  were used:  $T_N = 2.40$  K,  $2.25$  K, and  $2.15$  K. The  $S_S(Q, \omega; T)$  was determined by fitting it to the observed net scattering intensity,  $S_E(Q, \omega; T)$ , at  $T = 0.39$  K where  $f_S(T) = 1$ . In  $S_S(Q, \omega; T)$ ,  $S_1(Q, \omega; T)$  was represented by the usual damped harmonic oscillator (DHO) function:

$$S_1(Q, \omega; T) = \frac{Z_{Q,T}[n_B(\omega, T) + 1]}{\pi} \left\{ \frac{\Gamma_{Q,T}}{(\omega - \omega_{Q,T})^2 + \Gamma_{Q,T}^2} - \frac{\Gamma_{Q,T}}{(\omega + \omega_{Q,T})^2 + \Gamma_{Q,T}^2} \right\}, \quad (6)$$

where

$$n_B(\omega, T) \equiv \frac{1}{e^{\beta\hbar\omega} - 1} \quad (7)$$

is the Bose function.  $\omega_{Q,T}$ ,  $\Gamma_{Q,T}$ , and  $Z_{Q,T}$  are the energy, half width, and weight of the single phonon-roton excitation, respectively.

As noted, the component  $S_{SB}(Q, \omega)$  was obtained by fitting to the observed broad component at  $T = 0.39$  K. Given the precision of the present data and the fact that  $S_{SB}(Q, \omega)$  is small, we found that  $S_{SB}(Q, \omega)$  could also be represented by the broad scattering data at  $T_N$  in the normal phase accurately enough. To simplify the fitting procedure we therefore used  $S_{SB}(Q, \omega) = x S_E(Q, \omega; T_N)$ , where  $x$  is a scale factor determined by fitting to the data at  $T = 0.39$  K and held independent of  $T$ .

The fitting has been conducted as follows. We first obtain  $S_N(Q, \omega)$  as the observed data at  $T_N$ . Next, we fitted Eq. (2) [equivalent to Eq. (1) with  $f_S(T) = 1$ ] to the low-temperature data in the range  $0.3 \text{ meV} \leq \hbar\omega \leq 2.0 \text{ meV}$ . The four free parameters are  $x$ ,  $\omega_{Q,T}$ ,  $\Gamma_{Q,T}$ , and  $Z_{Q,T}$  and some examples of fits are shown in Fig. 4 and Fig. 5. For  $Q \geq 1.85 \text{ \AA}^{-1}$ , an additional component (fitted with a Gaussian) is detected in  $S_S(Q, \omega; T)$ . This component has been already detected in previous studies on helium in several porous media and has been identified as a 2D layer mode supported by the liquid layers close to the substrate surface.

We then fit the spectra at higher temperatures keeping  $x$  and  $Z_{Q,T}$  as fixed quantities and setting  $\Gamma_{Q,T}$  to the values found in literature for bulk helium.<sup>36,37</sup> In previous studies on helium confined in Vycor as well as in other porous materials,  $\Gamma_{Q,T}$  has been found to be the same as that in bulk helium. Thus, for  $0.4 \text{ K} < T < T_N$ , the free parameters are  $\omega_{Q,T}$  and  $f_S(T)$ .

In order to consider data with a reasonably strong singular component  $S_S(Q, \omega; T)$  as compared to the  $S_B(Q, \omega)$  component and to avoid the Q-range where the 2D component becomes observable, we focussed the analysis on the wave-vector range  $1.55 \text{ \AA}^{-1} \leq Q \leq 1.80 \text{ \AA}^{-1}$ . Examples of fits to data in this wave-vector range and for temperatures  $T = 1.80$  K to  $2.15$  K are shown in Figs. 6–9.

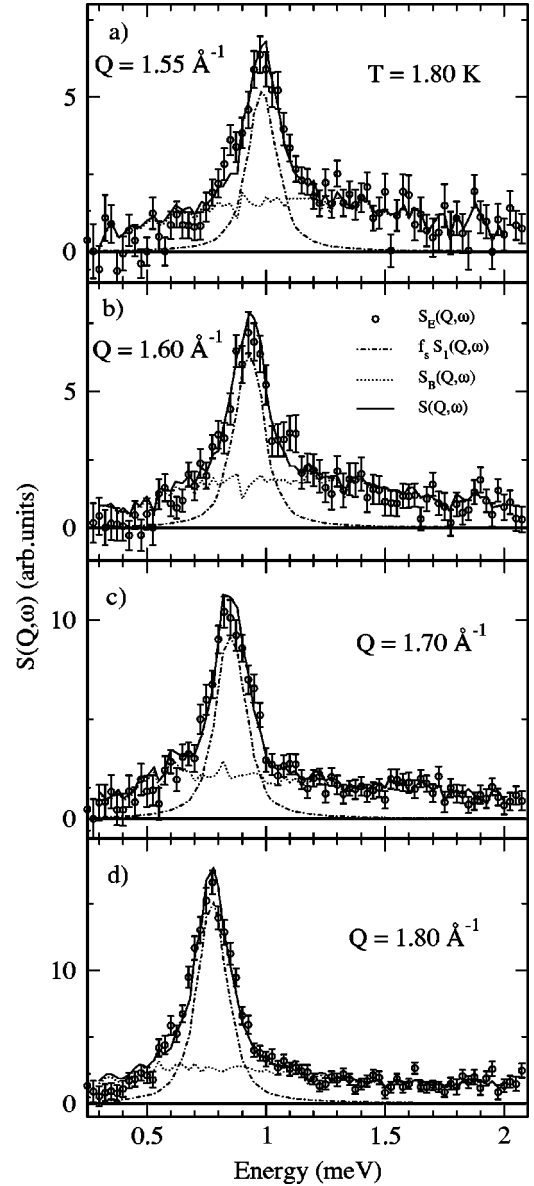
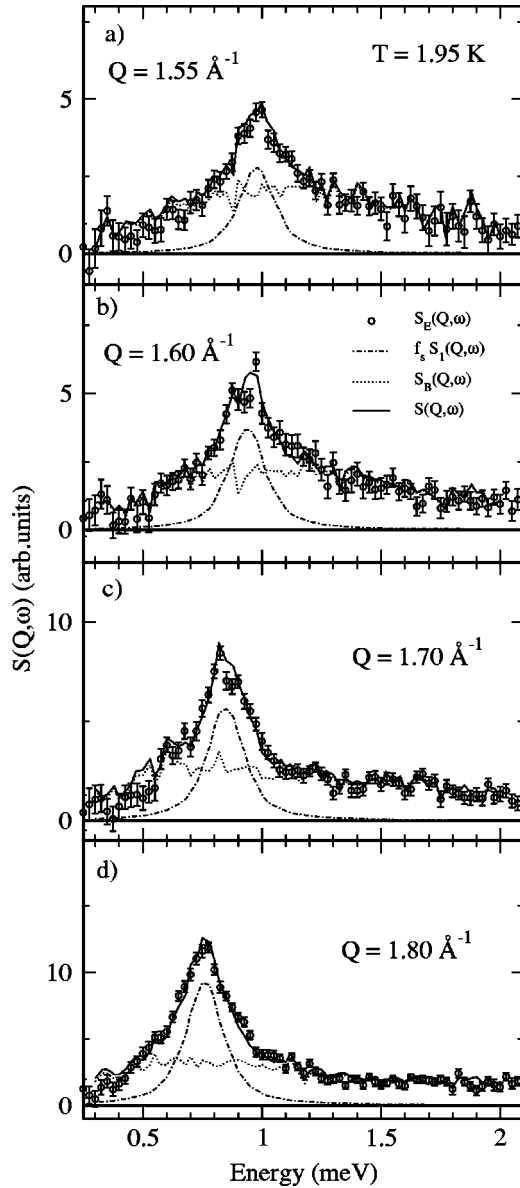


FIG. 6.  $S(Q, \omega; T)$  of liquid  $^4\text{He}$  in Vycor at  $T = 1.80$  K.  $S(Q, \omega; T)$  is represented as the sum of a single excitation component,  $f_S(T)S_1(Q, \omega; T)$ , plus a broad component  $S_B(Q, \omega; T)$  as in Eqs. (3) and (4).

#### IV. RESULTS

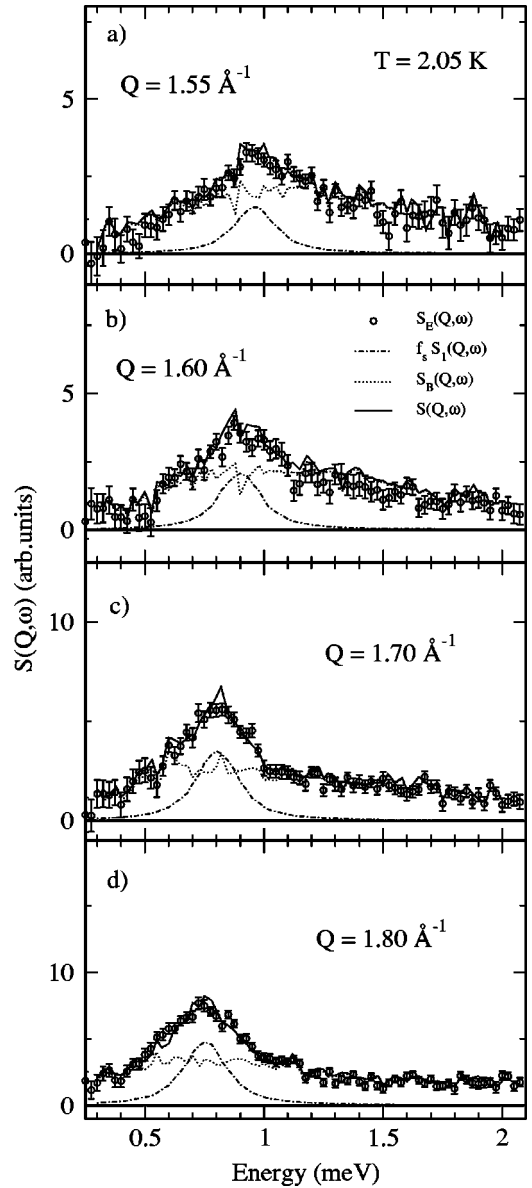
The observed dynamic structure factor,  $S(Q, \omega)$ , of superfluid  $^4\text{He}$  in Vycor at  $T = 0.39$  K is shown in Fig. 4 at four wave vectors. A well-defined phonon-roton mode in  $S(Q, \omega)$  is observed on top of a small, broad intensity. The width of the phonon-roton mode is set by the instrument resolution, here  $\approx 100 \mu\text{eV}$ . At each  $Q$ ,  $S(Q, \omega)$  is expressed as the sum of a single phonon-roton component,  $S_1(Q, \omega)$ , plus a broad component,  $S_{SB}(Q, \omega)$ , as in Eq. (2) which is fitted to the data. The resulting  $S_1(Q, \omega)$  and  $S_{SB}(Q, \omega)$  are shown in Fig. 4 as dot-dashed and dotted lines, respectively. At the roton wave vector,  $Q = 1.95 \text{ \AA}^{-1}$ , a gaussian component was also added to the fit to  $S(Q, \omega)$ . This represents the 2D layer mode that propagates in the liquid layers adjacent to the

FIG. 7. Same as Fig. 6, for  $T = 1.95$  K.

Vycor walls. This mode is observed with resolvable intensity for wave vectors near the roton  $Q$  only.

Figures 6–10 show  $S(Q, \omega; T)$  of liquid  ${}^4\text{He}$  in Vycor for wave vectors  $1.55 \text{ \AA}^{-1} \leq Q \leq 1.80 \text{ \AA}^{-1}$  and temperatures  $T = 1.80$ – $2.40$  K. In Fig. 6 we see a well-defined phonon-roton mode at  $T = 1.80$  K. The single phonon-roton component,  $S_1(Q, \omega; T)$ , of  $S(Q, \omega; T)$  is represented by the dashed-dotted line in Fig. 6. The total  $S(Q, \omega; T)$  is represented as  $S(Q, \omega; T) = f_S(T) S_1(Q, \omega; T) + S_B(Q, \omega; T)$  as given in Eqs. (3) and (4). As temperature increases, the weight  $f_S(T)$  in the single phonon-roton mode decreases until there is a small or absent phonon-roton mode weight in  $S(Q, \omega; T)$  at  $T = 2.15$  K (see Figs. 7–9). An important finding is that there is clearly a phonon-roton mode at  $T = 2.05$  K. At  $T = 2.25$  K, there is no observable phonon-roton mode in the data.

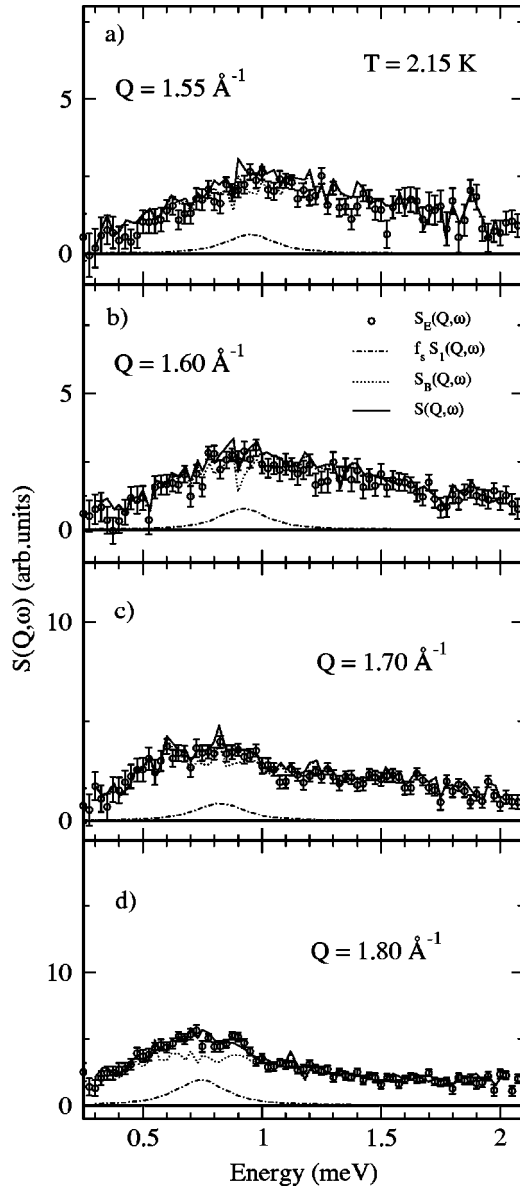
In the fitting of Eqs. (3) and (4) to the data, the phonon-roton energy  $\omega_{Q,T}$  and the weight  $f_S(T)$  are free parameters.

FIG. 8. Same as Fig. 6, for  $T = 2.05$  K.

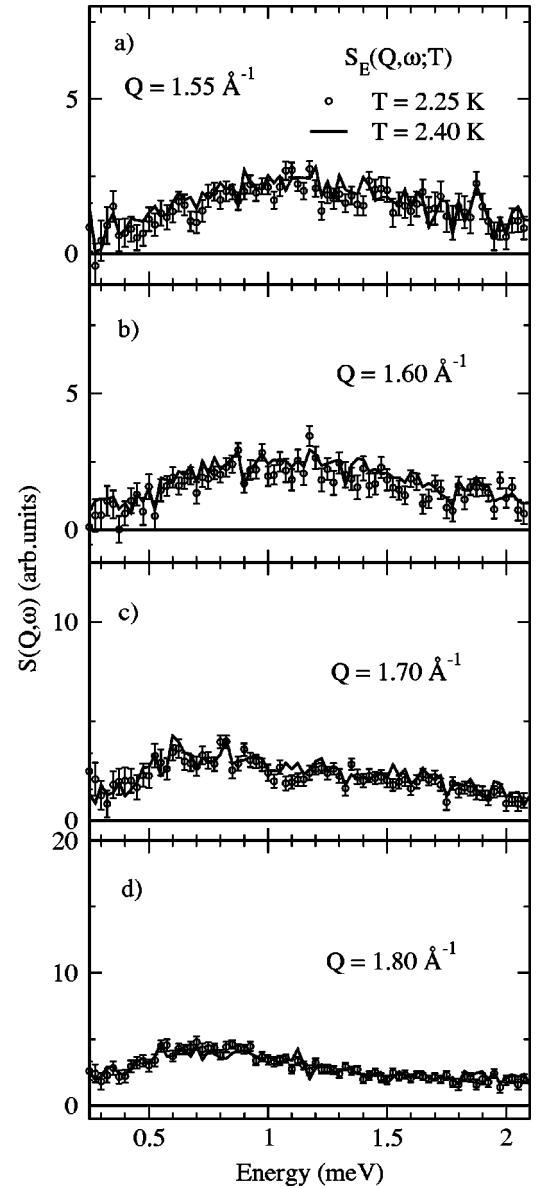
The resulting  $\omega_{Q,T}$  are shown in Fig. 11 along with the bulk superfluid  ${}^4\text{He}$   $\omega_{Q,T}$  at low  $T$ . The  $\omega_{Q,T}$  at low  $T$  in Vycor agree well with the bulk values at low  $T$  except that the Vycor  $\omega_{Q,T}$  are somewhat lower at  $Q = 1.55 \text{ \AA}^{-1}$  and somewhat higher at  $Q = 1.80 \text{ \AA}^{-1}$ . This suggests that the liquid density of liquid  ${}^4\text{He}$  in Vycor at partial fillings is somewhat lower than the bulk value.

Figure 12 shows the fraction  $f_S(T)$  of the weight of  $S(Q, \omega; T)$  that lies in the single phonon-roton mode for wave vectors  $1.55 \text{ \AA}^{-1} \leq Q \leq 1.85 \text{ \AA}^{-1}$  at four temperatures. Within the error of determination,  $f_S(T)$  is independent of  $Q$ . In the fitting of Eqs. (3) and (4) to the data to determine  $f_S(T)$ , the temperature  $T_N$  of the “normal” phase where  $f_S(T)$  must go to zero was taken as  $T_N = 2.40$  K. At each temperature shown in Fig. 12, the  $S(Q, \omega; T)$  was normalized by the amount of liquid in the Vycor,  $n_L = n_{\text{ads}} - n_{\text{cc}}$ .

Figure 13 shows the average of  $f_S(T)$  over the  $Q$  values depicted in Fig. 12.  $f_S(T)$  at temperatures between  $1.80$  K

FIG. 9. Same as Fig. 6, for  $T=2.15$  K.

and 2.15 K are shown. To test the sensitivity of  $f_S(T)$  to the value of  $T_N$  selected in the fitting,  $f_S(T)$  for three values of  $T_N$  are shown. Since  $f_S(T)$  must be zero at  $T_N$ , there is some dependence of  $f_S(T)$  on  $T_N$  at higher temperatures  $T$  approaching  $T_N$ . However, the basic finding for  $f_S(T)$  is independent of  $T_N$ , which is the fact that the weight  $f_S(T)$  in the single phonon-roton mode tracks  $\rho_s(T)$  in bulk liquid  $^4\text{He}$  much more closely than it does  $\rho_s(T)$  of  $^4\text{He}$  in Vycor. The solid line in Fig. 13 shows  $\rho_s(T)$  for bulk liquid  $^4\text{He}$ . The arrow shows  $T_c$  in the present sample of Vycor used to obtain the neutron-scattering data reported here. The present sample has a critical temperature  $T_c=2.05$  K where  $\rho_s(T_c)=0$ . Also shown is the  $\rho_s(T)$  observed by Chan *et al.*<sup>32</sup> in independent measurements on a different Vycor sample which has a  $T_c$  of  $T_c=1.95$  K. Zassenhaus and Reppy<sup>33</sup> have recently reported values of  $T_c$  of 2.03 K for Vycor. Clearly, there is some variation of  $T_c$  from sample to sample of Vycor. However,

FIG. 10.  $S(Q, \omega; T)$  of liquid  $^4\text{He}$  in Vycor at  $T > T_\lambda$ . Open symbols with error bars,  $T=2.25$  K; solid line,  $T=2.40$  K.

the  $T_c$  of the present Vycor sample for which  $f_S(T)$  is reported is  $T_c=2.05$  K.

From Fig. 13, we see that at  $T=2.05$  K where  $\rho_s(T)=0$  for the present sample, there is still a well-defined phonon-roton excitation. Indeed at  $T=2.05$  K nearly 40% of the intensity in  $S(Q, \omega; T)$  is in the phonon-roton mode [ $f_S(T) \approx 0.4$ ]. There appears to be a phonon-roton mode in Vycor at temperatures up to  $T \approx T_\lambda = 2.17$  K. The existence of a phonon-roton mode up to  $T \approx T_\lambda$  in Vycor suggests that there is a condensate in liquid  $^4\text{He}$  in Vycor above  $T_c$ , up to a temperature  $T \approx T_\lambda$ .

Finally, to test the sensitivity of  $f_S(T)$  to the normalization of the total  $S(Q, \omega; T)$ , we chose the normalizing liquid volume as  $n_L = n_{\text{ads}} - n_{\text{lay}}$  rather than  $n_L = n_{\text{ads}} - n_{\text{cc}}$ . The values of  $f_S(T)$  obtained using  $n_L = n_{\text{ads}} - n_{\text{lay}}$  are shown in Fig. 14. Comparing Figs. 13 and 14, we see that  $f_S(T)$  is not very



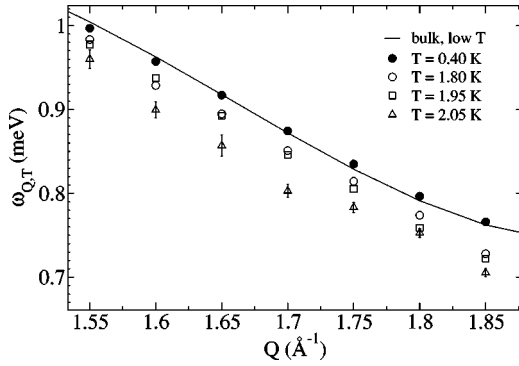


FIG. 11. Excitation energy  $\omega_{Q,T}$  in the  $Q$  range of interest for several temperatures; solid line indicates bulk values for low temperature. Results for  $T=2.05$  K show typical magnitude of error.

sensitive to the choice of  $n_L$  and the basic finding that there are well-defined phonon-rotons at higher temperatures  $T$  above  $T_c$  in Vycor is unchanged.

### V. DISCUSSION AND INTERPRETATION

The data presented here shows that liquid  $^4\text{He}$  in Vycor supports a single phonon-roton (P-R) excitation at temperatures above  $T_c=2.05$  K for wave vectors  $Q>1$   $\text{\AA}^{-1}$ . For example, a single P-R peak is observed in  $S(Q,\omega;T)$  for  $1.55\leq Q\leq 1.8$   $\text{\AA}^{-1}$  and  $T=2.05$  K as shown in Fig. 8. Since liquid  $^4\text{He}$  supports an observable P-R mode at higher  $Q$  because there is a condensate, this finding suggests that there is a condensate in liquid  $^4\text{He}$  in Vycor above  $T_c$ . This condensate is probably localized to favorable regions in the Vycor at temperatures above  $T_c$ . Neutron scattering is a local probe and can observe excitations supported in these islands of BEC. These islands of BEC are probably surrounded by regions of normal liquid.

To characterize the weight of the P-R mode in  $S(Q,\omega;T)$ , we fitted Eq. (3) to the observed  $S(Q,\omega;T)$ . In Eq. (3),  $S_1(Q,\omega;T)$  is the single P-R component. It is represented by a peaked function (a DHO function). The DHO has a temperature-dependent energy  $\omega_{Q,T}$  and half width  $\Gamma_{Q,T}$  but its weight  $Z_{Q,T}$  is held independent of  $T$ . Thus the weight of  $S_1(Q,\omega;T)$  in  $S(Q,\omega;T)$  as a function of temperature is

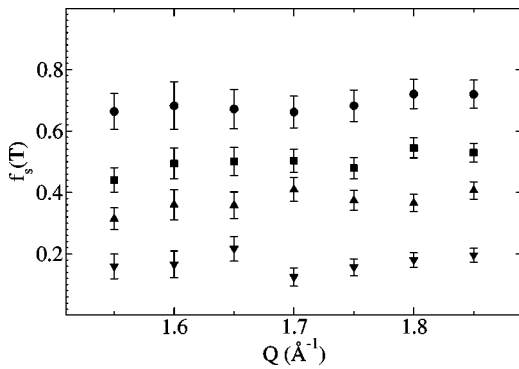


FIG. 12. Results for the fitting parameter  $f_s(T)$  when  $T_N=2.40$  K. Circles,  $T=1.80$  K; squares,  $T=1.95$  K; upward triangles,  $T=2.05$  K; and downward triangles,  $T=2.15$  K.

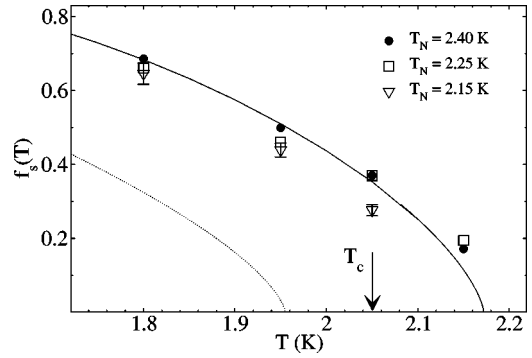


FIG. 13. Fitting parameter  $f_s(T)$  obtained as an average over the  $f_s(T)$  for the  $Q$  values shown in Fig. 12 for fitting schemes described in the text (using  $n_L=n_{\text{ads}}-n_{\text{cc}}$  and several  $T_N$ ). The solid and dotted lines show the superfluid fraction for bulk superfluid  $^4\text{He}$  (Refs. 39, 38) and for  $^4\text{He}$  confined in Vycor (Ref. 32), respectively. The arrow shows the superfluid to normal fluid transition temperature,  $T_c$ , for the present Vycor sample (see Sec. II D).

carried entirely by  $f_s(T)$ .  $S_B(Q,\omega;T)$  is a temperature dependent, broad function of  $\omega$  defined above in Eq. (4) which represents the broad components of  $S(Q,\omega;T)$ . Fits of Eq. (3) to the data yield the weights  $f_s(T)$  of  $S_1(Q,\omega;T)$  in  $S(Q,\omega;T)$  shown in Figs. 13 and 14. These figures show that  $f_s(T)$  goes to zero at  $\approx T_\lambda=2.17$  K rather than at  $T_c=2.05$  K. Indeed  $f_s(T)$  scales with  $T$  approximately as  $\rho_s(T)$  in bulk liquid  $^4\text{He}$ . Since, as noted above, an observable P-R mode at higher  $Q$  arises because there is a condensate, this scaling is interpreted as showing that there is a condensate in Vycor above  $T_c$  and up to  $\approx T_\lambda$ . Certainly,  $f_s(T)$  in Vycor does not scale as  $\rho_s(T)$  in Vycor. In bulk liquid  $^4\text{He}$ , the  $f_s(T)$  is generally found to scale approximately as  $\rho_s(T)$  for the bulk as well and all the indications are that the condensate fraction  $n_0(T)$  and  $\rho_s(T)$  in bulk liquid  $^4\text{He}$  go to zero at the same temperature  $T_\lambda$ .

Other fitting procedures are possible. The chief difference between the present and other procedures is the choice of the “broad” function  $S_B(Q,\omega;T)$ . Provided the DHO and  $S_B(Q,\omega;T)$  are sufficiently different, the same general dependence of  $f_s(T)$  on temperature would be obtained in other procedures as found here.

The above findings are interpreted as follows. Liquid  $^4\text{He}$

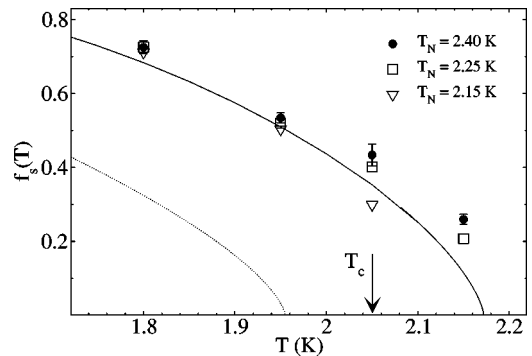


FIG. 14. Same as Fig. 13, for fitting schemes described in the text (using  $n_L=n_{\text{ads}}-n_{\text{lay}}$  and several  $T_N$ ).

in Vycor above  $T_\lambda$  is interpreted as a completely normal fluid (no BEC, no superflow). As in bulk liquid  $^4\text{He}$ ,  $S(Q, \omega; T)$  for  $Q \geq 1 \text{ \AA}^{-1}$  in Vycor above  $T_\lambda$  is a broad, featureless function of  $\omega$  which changes little with further increase in  $T$ . As  $T$  is lowered through  $T_\lambda$ , BEC begins to take place in favorable regions in the Vycor (e.g., in the larger pore volumes). For temperatures  $T$ ,  $T_c \leq T \leq T_\lambda$ , the regions supporting a condensate are separated by regions of normal fluid. The normal regions will be in the smaller pores, in irregular regions or in pores containing debris. The islands of BEC probably have length scales of order 30–50  $\text{\AA}$ . At least they must be large enough to support an excitation of wave length of  $\approx 10 \text{ \AA}$ . There will be phase coherence within the islands of BEC. As  $T$  is lowered further below  $T_\lambda$ , the dimensions of the regions of BEC increase until at  $T_c$  the islands coalesce. At  $T_c$  there is phase coherence across the whole sample and superflow across the whole sample can be observed as in a torsional oscillator experiment or as in a measurement of sound velocity across the whole sample as made here to determine  $T_c$ .

Models of BEC and superfluidity in disorder and of superconductivity in disorder suggest the above picture. Huang and Meng<sup>3</sup> examine both BEC and superfluidity in a Bose gas in disorder. For white-noise disorder introduced by point

impurities randomly distributed in the gas, they and others<sup>6,8,9,40</sup> find that the superfluid density is suppressed more by disorder than is the condensate fraction. In an important paper, Astrakharchik, Boronat, Casulleras, and Giorgini<sup>8</sup> extend these results to liquid densities and strong disorder using Monte Carlo methods. They find that the superfluid density can be driven to zero by the disorder while the condensate fraction can remain finite. For a Bose gas in disorder, Lopatin and Vinokur<sup>9</sup> propose that there are regions in temperature where there is BEC but no superfluidity. Similarly there are models of superconductivity in high- $T_c$  materials (disordered materials) which display regions of superconductivity separated by normal regions.<sup>18</sup> These are regions of finite-energy gap separated by regions of zero energy gap. The above picture also has analogies with Josephson-junction arrays.<sup>23,24</sup>

### ACKNOWLEDGMENTS

It is a pleasure to acknowledge valuable discussions with B. Fåk and J. Z. Larese. Partial support by the National Science Foundation (USA) Grant No. DMR-0115663 is gratefully acknowledged.

\*Electronic address: albergam@ill.fr

†Electronic address: glyde@udel.edu

‡Electronic address: 19218@udel.edu

§Electronic address: mulders@udel.edu

||Electronic address: bossy@grenoble.cnrs.fr

\*Electronic address: schober@ill.fr

<sup>1</sup>M.P.A. Fisher, P.B. Weichman, G. Grinstein, and D.S. Fisher, Phys. Rev. B **40**, 546 (1989).

<sup>2</sup>W. Krauth, N. Trivedi, and D. Ceperley, Phys. Rev. Lett. **67**, 2307 (1991).

<sup>3</sup>K. Huang and H.-F. Meng, Phys. Rev. Lett. **69**, 644 (1992).

<sup>4</sup>J.D. Reppy, J. Low Temp. Phys. **87**, 205 (1992).

<sup>5</sup>M. Ma, P. Nisamaneephong, and L. Zhang, J. Low Temp. Phys. **93**, 957 (1993).

<sup>6</sup>S. Giorgini, L. Pitaevskii, and S. Stringari, Phys. Rev. B **49**, 12 938 (1994).

<sup>7</sup>K. Huang, in *Bose-Einstein Condensation*, edited by A. Griffin, D. Snoke, and S. Stringari (Cambridge University Press, Cambridge, 1995).

<sup>8</sup>G.E. Astrakharchik, J. Boronat, J. Casulleras, and S. Giorgini, Phys. Rev. A **66**, 023603 (2002).

<sup>9</sup>A.V. Lopatin and V.M. Vinokur, Phys. Rev. Lett. **88**, 235503 (2002).

<sup>10</sup>G. Coddens, J.D. Kinder, and R. Millet, J. Non-Cryst. Solids **188**, 41 (1995).

<sup>11</sup>R.M. Dimeo, P.E. Sokol, C.R. Anderson, W.G. Stirling, K.H. Andersen, and M.A. Adams, Phys. Rev. Lett. **81**, 5860 (1998).

<sup>12</sup>O. Plantevin, B. Fåk, H.R. Glyde, J. Bossy, and J.R. Beamish, Phys. Rev. B **57**, 10 775 (1998).

<sup>13</sup>C.R. Anderson, K.H. Andersen, J. Bossy, W.G. Stirling, R.M. Dimeo, P.E. Sokol, J.C. Cook, and D.W. Brown, Phys. Rev. B **59**, 13 588 (1999).

<sup>14</sup>B. Fåk, O. Plantevin, H.R. Glyde, and N. Mulders, Phys. Rev. Lett. **85**, 3886 (2000).

<sup>15</sup>H.R. Glyde, O. Plantevin, B. Fåk, G. Coddens, P.S. Danielson, and H. Schober, Phys. Rev. Lett. **84**, 2646 (2000).

<sup>16</sup>B. Fåk and H. R. Glyde, in *Advances in Quantum Many-Body Theory*, edited by E. Krotscheck and J. Navarro (World Scientific, Singapore, 2002), Vol. 4.

<sup>17</sup>C.R. Anderson, K.H. Andersen, W.G. Stirling, P.E. Sokol, and R.M. Dimeo, Phys. Rev. B **65**, 174509 (2002).

<sup>18</sup>N. Trivedi, A. Ghosal, and M. Randeria, Int. J. Mod. Phys. B **15**, 1347 (2001).

<sup>19</sup>G. Blatter, M.V. Feigel'man, V.B. Geshkenbein, A.I. Larkin, and V.M. Vinokur, Rev. Mod. Phys. **66**, 1125 (1994).

<sup>20</sup>U.C. Tauber and D.R. Nelson, Phys. Rep. **289**, 157 (1997).

<sup>21</sup>A. van Otterlo, R.T. Scalettar, and G.T. Zimanyi, Phys. Rev. Lett. **81**, 1497 (1998).

<sup>22</sup>N. Marković, C. Christiansen, A.M. Mack, W.H. Huber, and A.M. Goldman, Phys. Rev. B **60**, 4320 (1999).

<sup>23</sup>M.G. Forrester, S.P. Benz, and C.J. Lobb, Phys. Rev. B **41**, 8749 (1990).

<sup>24</sup>A. van Otterlo, K.H. Wagenblast, R. Fazio, and G. Schon, Phys. Rev. B **48**, 3316 (1993).

<sup>25</sup>K. Sheshadri, H.R. Krishnamurthy, R. Pandit, and T.V. Ramakrishnan, Phys. Rev. Lett. **75**, 4075 (1995).

<sup>26</sup>O. Plantevin, B. Fåk, H.R. Glyde, N. Mulders, J. Bossy, G. Coddens, and H. Schober, Phys. Rev. B **63**, 224508 (2001).

<sup>27</sup>O. Plantevin, H.R. Glyde, B. Fåk, J. Bossy, F. Albergamo, N. Mulders, and H. Schober, Phys. Rev. B **65**, 224505 (2002).

<sup>28</sup>H. R. Glyde, O. Plantevin, B. Fåk, and J. Bossy, in Proceedings of ILL Millennium Symposium (SCO, ILL, Grenoble, France, 2001) (unpublished), p. 91.

<sup>29</sup>R.T. Azuah, H.R. Glyde, R. Scherm, N. Mulders, and B. Fåk, J. Low Temp. Phys. **130**, 557 (2003).

- <sup>30</sup>F. Albergamo, J. Bossy, H.R. Glyde, and A.-J. Dianoux, *Phys. Rev. B* **67**, 224506 (2003).
- <sup>31</sup>N. Mulders and J.R. Beamish, *Phys. Rev. Lett.* **62**, 438 (1989).
- <sup>32</sup>M.H.W. Chan, K.I. Blum, S.Q. Murphy, G.K.S. Wong, and J.D. Reppy, *Phys. Rev. Lett.* **61**, 1950 (1988).
- <sup>33</sup>G.M. Zassenhaus and J.D. Reppy, *Phys. Rev. Lett.* **83**, 4800 (1999).
- <sup>34</sup>A.D.B. Woods and E.C. Svensson, *Phys. Rev. Lett.* **41**, 974 (1978).
- <sup>35</sup>H. R. Glyde, *Excitations in Liquid and Solid Helium* (Clarendon Press, New York, 1994).
- <sup>36</sup>K.H. Andersen and W.G. Stirling, *J. Phys.: Condens. Matter* **6**, 5805 (1994).
- <sup>37</sup>K.H. Andersen, W.G. Stirling, R. Scherm, A. Stunault, B. Fåk, H. Godfrin, and A.-J. Dianoux, *J. Phys.: Condens. Matter* **6**, 821 (1994).
- <sup>38</sup>D.S. Greywall and G. Ahlers, *Phys. Rev. A* **7**, 2145 (1973).
- <sup>39</sup>J. Maynard, *Phys. Rev. B* **14**, 3868 (1976).
- <sup>40</sup>M.C. Gordillo and D.M. Ceperley, *Phys. Rev. Lett.* **85**, 4735 (2000).